Appl. Phys. B (2015) 121:363–368
DOI 10.1007/s00340-015-6238-2

Applied Physics B
Lasers and Optics

Femtosecond filament array generated in air

Acner Camino[1] · Tingting Xi[2] · Zuoqiang Hao[1] · Jingquan Lin[1]

Received: 30 May 2015 / Accepted: 30 September 2015 / Published online: 22 October 2015

Abstract Patterning multiple filamentation of femtosecond pulses in air is studied using a microlens array for modulation of the spatial profile and a single lens for power concentration. We generate a stable array of filaments containing a maximum of five hotspots per mm^2 from a modest 68-GW input power. The evolution of the pattern along the axis of propagation as well as the means to control the inter-filament spacing is discussed. It is also shown in numerical simulations that besides the filamentation in the proximities of the focus, there is a region of early ionization around the central hotspots in the beam profile and a revival afterwards, caused by the spatial distribution of the laser energy.

1 Introduction

Femtosecond laser pulses propagating through air and carrying a power higher than a certain threshold experience a number of nonlinear effects that eventually lead to self-guided filaments [1]. The fundamental physical events that take place in the formation of filaments are the initiation of the converging Kerr effect and the following counteracting phenomena that prevent the collapse of the beam, namely plasma defocusing, chromatic dispersion, higher-order terms of the Kerr effect and ultimately natural diffraction. Many applications of this special form of light propagation have emerged in the last decade, utilizing filaments for the generation of supercontinuum [2], guidance of electric discharges [3], generation of THz radiation [4] or laser-induced water condensation [5]. It is also known that in the propagation of pulses of power much higher than the critical value for self focusing, the local nonlinearity 'saturates,' clamping the intensity to a certain maximum value at approximately 5×10^{13} W/cm^2. As a result, when pulses of a much higher power propagate, multiple filaments appear [6]. Motivated by this phenomenon, several works over the past years have been dedicated to govern the multiple filamentation (MF) over the action of noise, in order to obtain organized and reproducible distributions, especially after the development of tera- and peta-watt ultrashort laser facilities around the world. The realization of a tailored array of filaments has interesting potential applications like improving the guidance of electric discharges [7], generation of mJ-level supercontinuum in solid media [8], or the formation of instantaneous waveguides for infrared [9], visible [10] and microwave radiation in the air [11].

The earliest works that achieved deterministic control of MF patterns were performed in dielectric media, utilizing various techniques [12–19] to control the spatial profile of the incident beam. They used media with high nonlinearity that allowed the generation of a considerable amount of filaments without necessitating TW-level lasers. In the report by Méchain et al. [20], it was demonstrated the organization of the MF pattern in air regulated by the diffraction after the laser propagation through an iris. Other works have effectively optimized the MF in air by varying the aperture of a pinhole [21], by the densification

✉ Tingting Xi
ttxi@ucas.ac.cn

Zuoqiang Hao
zqhao@cust.edu.cn

Jingquan Lin
linjingquan@cust.edu.cn

[1] School of Science, Changchun University of Science and Technology, Changchun 130022, China

[2] School of Physics, University of Chinese Academy of Sciences, Beijing 101407, China

of the laser power into a smaller beam diameter [22] or by modifying the beam profile using a modulated liquid surface acting as a mirror [23]. Moreover, the work published in Ref. [24] demonstrated the use of deformable mirrors controlled by actuators as spatial phase shapers in deterministic MF. The main appeal of the optics employed in Refs. [23, 24] is their efficient use of the available power by utilizing reflective optics with adjustable focusing power and pitch.

Deterministic MF in air aims to control three fundamental features of the filament: their characteristics in the transversal plane (filament number, separation and diameter), their capacity to survive propagation (control of the filaments length) and the electron density distribution of the resulting plasma in the transversal plane and over the propagation axis. In the present work, we provide a power efficient scheme that achieves deterministic control of MF in air by using a microlens array (MLA) to modulate the spatial profile of the beam first and then a conventional plano-convex lens placed at a variable distance from MLA, to concentrate the laser light near the focus. The action of a deformable liquid mirror in Ref. [23] and a MLA for spatial phase modulation is relatively similar, each of them having their relative advantages and disadvantages for MF. The first of them makes a more efficient use of the available power due to its reflective nature, at the expense of being more costly and complex to implement experimentally. The MLA on the other hand can provide diffraction patterns with a higher number of hotspots, beneficial in applications such as laser-induced surface ablation or in the manipulation of the features of previously proposed models for instantaneous plasma waveguides [9].

We prove in this work that effective generation of filaments in air is achievable after propagation through a transmitting phase element (MLA) and posterior conventional focusing of the resulting diffraction pattern, in a simple setup utilizing a modest power laser. The addition of a single lens enhances the capability of plasma generation from a beam formed by a highly dense diffraction pattern (such as in Refs. [16–18]) in a medium with a low nonlinearity such as air. In addition, we discuss the characteristics of air ionization along the propagation axis under the current focusing scheme. Our simulations show that besides filamentation near the focus, there is early ionization of the medium and revivals afterwards. Effective manipulation of the hot spot separation is also fundamental for a completely controlled tailoring of an array of filaments in any medium. In this work, we demonstrate that the issue of controlling the filament-to-filament distance is effectively addressed by altering the pitch of the phase element.

2 Experiments and discussion

The light source utilized in this experiment is a Libra system (Coherent Inc.,) that provides Gaussian pulses centered at 800 nm, pulse width 50 fs and power 3.4 W at a 1 kHz repetition rate, representing a peak power of 68 GW. The laser beam will firstly meet a phase element consisting of a 10 × 10 array of microlenses (pitch = 1.015 mm, $f = 218.3$ mm, Edmund optics) which modulates the spatial profile at $z = 0$. Then, a converging lens (L_1) of focal length $f = 500$ mm is placed 0.5 m after the MLA array for concentration of the light to allow filamentation. Therefore, we will study the spatial profile and electron density of the MF generation in the proximities of $z = 1.0$ m.

A sound emerging from the focal region can be clearly heard [25], and an obvious spectral broadening can be observed in Fig. 1k, consequence of the action of nonlinear effects in the central spots. The hotspot pattern variation along the propagation axis is recorded by single-pulse illumination of a photosensitive paper and is shown in Fig. 1. On Fig. 1a–h, it is shown the distribution of the hotspots initially formed by linear diffraction, at eight positions before and after the focus of L_1. Figure 1i, j represents the simulated cross section at $z = 1.0$ m and the calculated maximum electron density along the z-axis obtained from numerically propagating the coupled nonlinear Schrödinger equations as explained in Ref. [26]. The coupled nonlinear Schrödinger equations are written as:

$$\begin{aligned}\frac{\partial E}{\partial z} &= i\frac{1}{2k_0}\nabla_\perp^2 E - i\frac{k''}{2}\frac{\partial^2}{\partial t^2}E \\ &\quad + ik_0 n_2\left[\frac{1}{2}\left(|E|^2 + \tau_{\mathrm{k}}^{-1}\int_{-\infty}^{t} \mathrm{e}^{-(t-t')/\tau_k}\left|E(t')\right|^2 \mathrm{d}t'\right)\right]E \\ &\quad - ik_0\frac{n_{\mathrm{e}}}{2n_{\mathrm{c}}}E - \frac{1}{2}\beta^{(K)}|E|^{2K-2}E, \end{aligned} \tag{1}$$

$$\frac{\partial n_{\mathrm{e}}}{\partial t} = \frac{\beta^{(K)}}{K\hbar\omega_0}|E|^{2K}\left(1 - \frac{n_{\mathrm{e}}}{n_{\mathrm{at}}}\right), \tag{2}$$

where E is the electric field envelope for the laser pulse with central wavelength $\lambda_0 = 800$ nm, $k_0 = 2\pi/\lambda_0$ is the central wave number, and z is the propagation distance. In the propagation equation, several effects are considered. The transverse diffraction is described by the Laplacian operator $\nabla_\perp^2$. The group-velocity dispersion is considered with the coefficient $k'' = 0.2$ fs^2/cm. The Kerr effect is composed of an instantaneous contribution with the coefficient $n_2 = 4 \times 10^{-19}$ cm^2/W and a delayed part with the relaxation time $\tau_{\mathrm{k}} = 70$ fs. The electron defocusing effect and the multiphoton absorption with the ionization coefficient of oxygen $\beta^{(K)} = 3.1 \times 10^{-98}$ cm^{13}/W^7 for the number $K = 8$

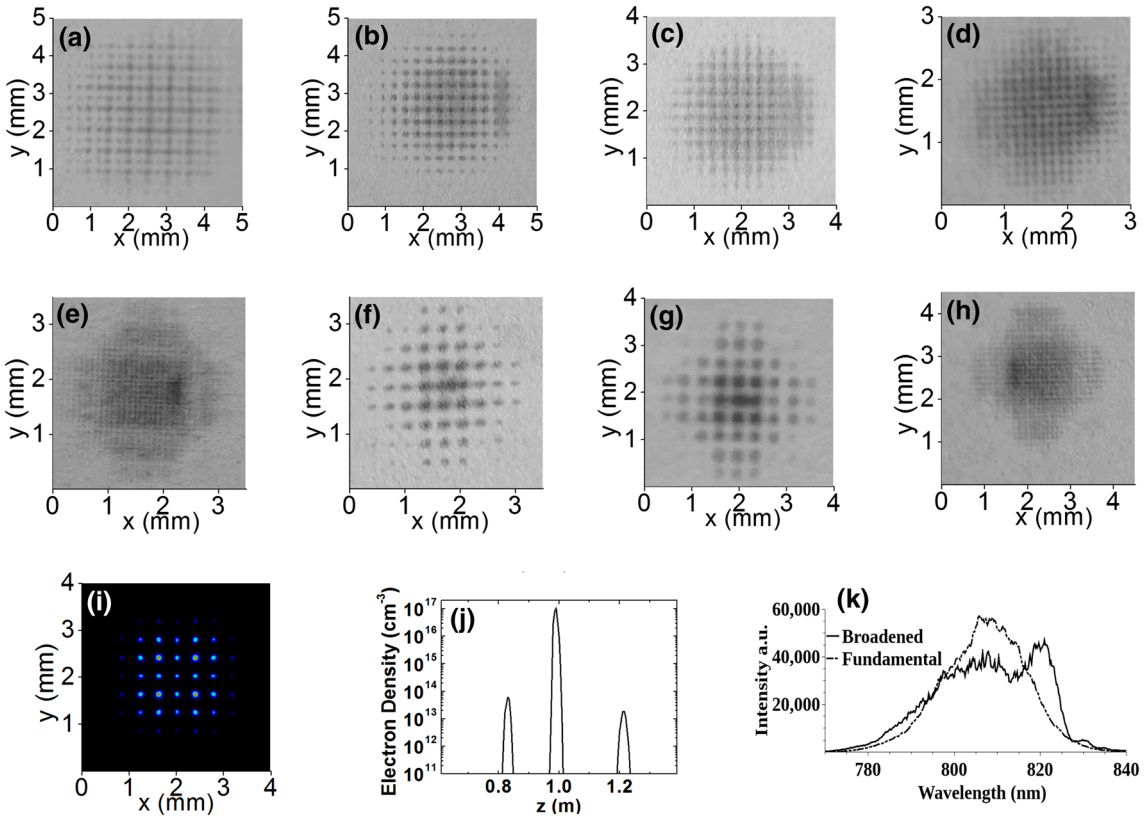

Fig. 1 **a**–**h** *Grayscale* pictures of the hotspot distribution after 0.7 m (**a**), 0.83 m (**b**), 0.88 m (**c**), 0.93 m (**d**), 0.975 m (**e**), 1.00 m (**f**), 1.025 m (**g**) and 1.05 m (**h**) from the MLA. In **i** it is plotted the simulated hotspot distribution at the focus of L_1 and in **j** the electron density along the propagation axis. In **k** it is shown the spectral broadening caused by filamentation in the central hotspots

are also included. In addition, the critical plasma density and the neutral oxygen density are $n_c = 1.7 \times 10^{21}$ cm^{-3}, $n_{at} = 5.4 \times 10^{18}$ cm^{-3}, respectively.

The incident field of the laser pulse is described by the Gaussian profile, which is written as:

$$E = \sqrt{2P_{in}/\pi w_0^2}\exp\left(-\frac{x^2+y^2}{w_0^2} - \frac{t^2}{\tau_0^2}\right), \tag{3}$$

where the transverse waist $w_0 = 4$ mm and the pulse duration (FWHM) $\Delta T = \sqrt{2\ln 2}\tau_0 = 50$ fs. The initial energy of the laser pulse is 3.4 mJ corresponding to the peak power $P_{in} = 68$ GW. The initial pulse is focused by the MLA with pitch $= 1$ mm and $f = 220$ mm. Then, a converging lens with a focal length $f = 500$ mm is placed at $z = 0.5$ m.

It is observed in the evolution from Fig. 1a–h that the hotspot distribution and their separation change within the transversal pattern along the propagation axis. The evolving beam contains at any point a number of hotspots higher than the number of elements in the MLA, an indicator of the action of diffraction in the tailoring of the MF pattern [27]. An inspection of the beam profile transformation reveals that the role of diffraction under this scheme is more complex than what it is usually considered in normal focusing geometries. Note that from the beginning of the propagation, intense spots of a small diameter begin to appear before the pulse arrives to the focal region corresponding to L_1. According to the calculations shown in Fig. 1j, at positions around $z = 0.83$ m their intensity is high enough for ionization. Despite this, early plasma divergence and ionization loss will not prevent the beam from forming filaments in the proximities of the focus. Also, regardless of the fact that Kerr effect around the most intense hotspots determines the positions where filaments will form, diffraction-induced unequal distribution of the energy to the hotspots formed due to the Talbot effect [27] is what ultimately establishes in a very deterministic way the position of the strongest hotspots in the pattern, influencing the number of filaments. In Fig. 1, there are a total of over 60 hotspots forming the pattern, corresponding to a density of five hotspots/mm^2. After this region, propagation is dominated by diffraction again; however, revival of the filamentation of the central spots is possible because after the termination of filaments, the diverging beam profile

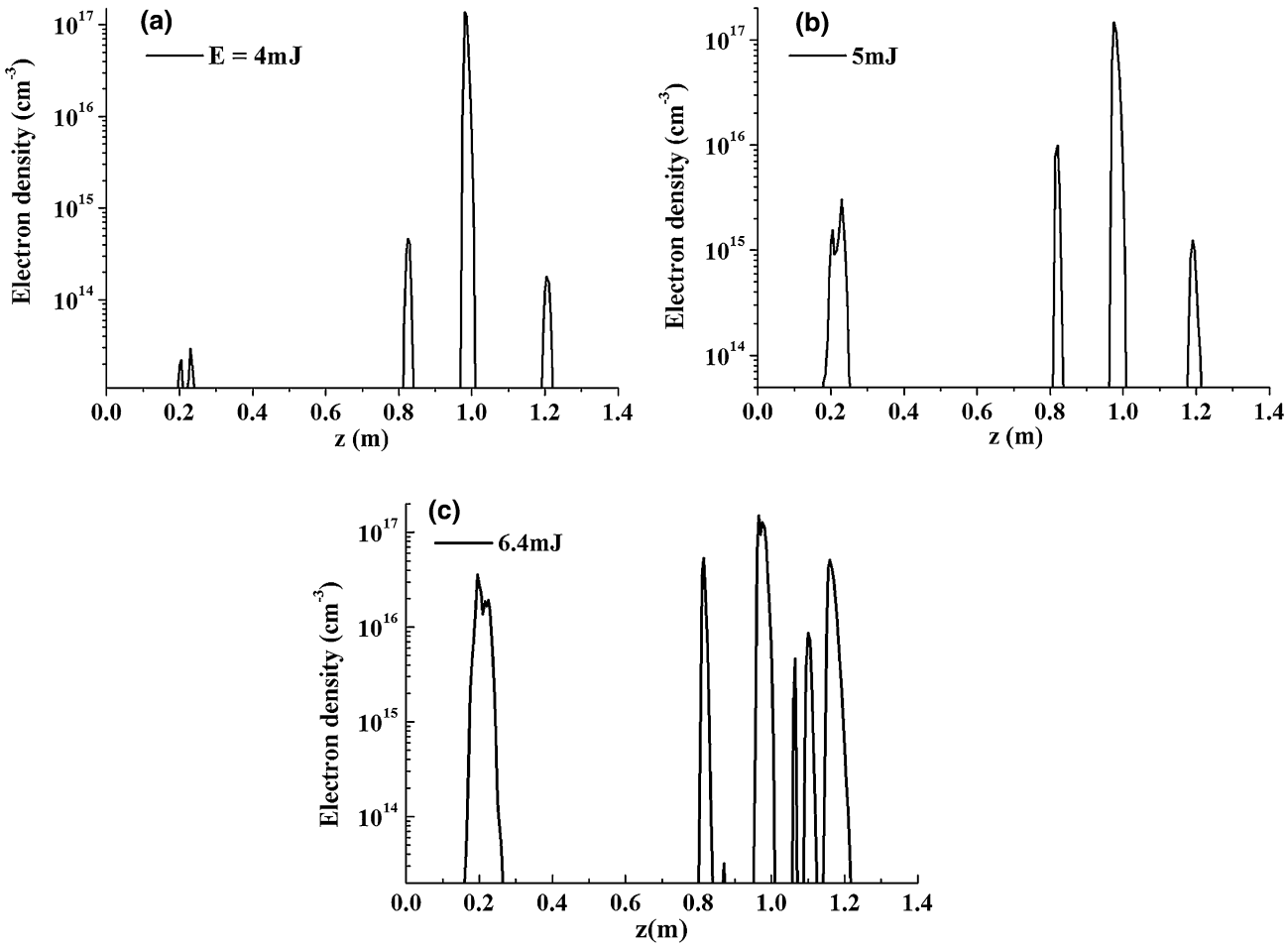

Fig. 2 Evolution of the maximum electron density along the axis of propagation for input energies of 4 mJ (**a**), 5 mJ (**b**) and 6.4 mJ (**c**)

still maintains a structure of hotspots, favoring the posterior action of the Kerr effect. The results shown in Fig. 1 demonstrate that this focusing geometry has the potential to support a high number of stable filaments organized by diffraction, even with a modest incident power.

As it was observed in Fig. 1j, early (and weak) plasma generation appears before the pulse arrives to the focal region at $z = 1.0$ m. This behavior is not surprising, considering that Kerr effect will act naturally around hotspots on the beam's spatial profile, as long as they carry a power that reaches a certain threshold. In order to evaluate the importance of this early ionization, in Fig. 2, we have calculated the evolution of the medium ionization over the pulse propagation axis at different incident laser pulse energies.

In Fig. 2, we observe that for higher energies a buildup of ionization in the proximities of the MLA focus ($z = 0.218$ m) begins to appear, as expected. Besides this one and the main ionization around the focus of L_1, two additional regions of medium ionization (before and after $z = 1.0$ m) are found in all cases [28], all of them containing an organized distribution of hotspots. Paying close attention to the results of the calculations in Figs. 1j and 2, it can be confirmed that increasing of the pulse energy, despite the fact that early ionization in the proximities of $z = 0.83$ m becomes stronger, plasma-induced divergence does not result in a shortening of the main filamentation region in the proximities of the focus. In addition, it is interesting to note that although the regions of medium ionization after $z = 1.0$ m are larger for higher incident energies, they do not appear to form a continuous plasma channel in Fig. 2c. In this respect, Ref. [29] has proved before the effectiveness of introducing a weak astigmatism in increasing the length of filaments. Therefore, astigmatic focusing of the multi-spot pattern with L_1 might constitute a promising method for the generation of long laser-induced multiple plasma channels by merely manipulating the focusing conditions of a femtosecond pulse.

Keeping in sight the promising atmospheric applications of MF, such as guiding in the propagation of infrared and microwave radiation, it is very important to study the means to deterministically tune the spacing between individual filaments in a MF pattern. In this regard, it is a

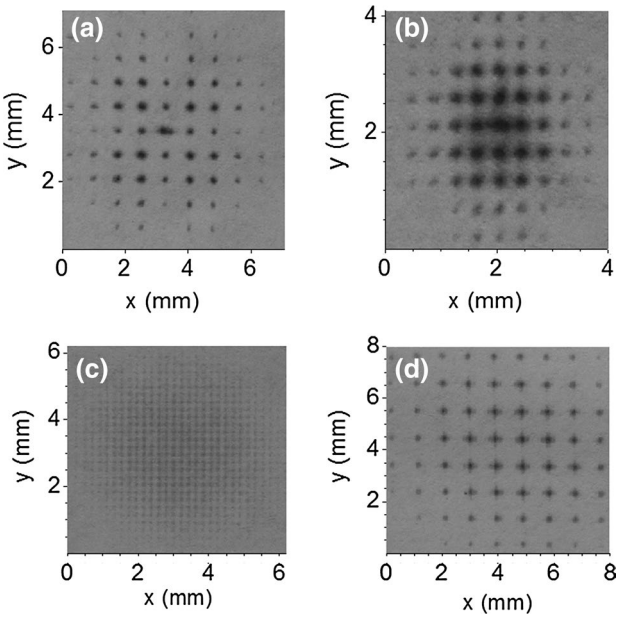

Fig. 3 Patterns of hotspots recorded in photosensitive paper at the foci corresponding to L_1 using a MLA with pitch 0.5 mm in **a** and 1.015 mm in **b**. Patterns at the MLA focus are, respectively, depicted in **c**, **d**

known phenomenon that when focusing the diffraction pattern emerging from a grating with a normal lens, a version of the diffractive element is created on the Fourier plane. Considering that the focal plane of the MLA contains a two-dimensional array of individual light sources, we can observe the effect that modifying the MLA element has in the inter-filament distance by observing the transformation of the pattern on a photosensitive paper placed at L_1's Fourier plane. The patterns generated after single-shot irradiation are shown in Fig. 3.

Figure 3a, b shows the patterns formed by single shot in the Fourier plane corresponding to L_1, while Fig. 3c, d corresponds to the patterns at the focus of the two MLA, respectively. In both cases the distance from the focal plane of the MLA to the lens L_1 was kept at 500 mm. We can observe that while the number of spots intense enough to cause change of color of the photosensitive paper in both cases is very similar (between 65 and 68 spots), the distance between consecutive spots is 2.4 times bigger in the case where the small-pitch MLA is used. Given that Fig. 3c, d is a pattern with similar shape and number of spots in Fig. 3a, b, we can note that it is not the microlens size itself but instead its numerical aperture is what determines a higher spot separation in the filamentation region. Notice here that the divergence of the MLA element in Fig. 3c is bigger (0.25°) than the one corresponding to Fig. 3d, which is 0.1°, forming a bigger beam size at the focus of L_1 in the first case, where filaments will be separated by a greater distance. A proper tuning of the inter-filamentation distance is especially important in applications when long-distance propagation without interaction between consecutive filaments is desired, since it is known from previous works [22, 30] that there is a saturation limit to the number of filaments in a MF pattern.

It must be argued as well that the relative distance between MLA and L_1 is not irrelevant to the MF pattern. It is known that as the beam propagates after passing the MLA element, a myriad of patterns of hotspots known as Talbot effect [27] appears due to the redistribution of the energy in the plane transversal to the propagation axis. Therefore, imaging different patterns by placing L_1 at different points along this axis can favor certain spots in the pattern at the expense of others. Finally, we need to point out that there is still an obvious second way of effectively modifying the inter-filament separation: to change the focal of the lens L_1 and hence modify the numerical aperture of the main focusing element, resulting in a modification of the beam size at the filamentation region.

3 Conclusions

We have achieved high-density deterministic MF from a modest GW femtosecond laser in air. The scheme proposed is spatial profile modulation for control of the hotspot distribution in the spatial profile and focusing of the resulting diffraction pattern in order to concentrate the available power. We have also proved the feasibility of controlling the inter-filament distance in the atmosphere by modifying the focusing conditions. We have found that the use of a greater numerical aperture MLA element for modulation of the pre-focused spatial profile reduces the density of filaments in the pattern and increases their diameter. In all cases, early ionization of the medium occurs before the focal region and revivals after the termination of filaments due to Kerr effect contribution around the hotspots in spatial profile of the beam, keeping always an organized distribution of filaments. Finally, the inter-filament distance proved to be independent from the MLA-lens relative distance, while it is strongly dependent on the MLA numerical aperture and the focal length of the single lens. This suggests that the dynamics determining the MF distribution in this work also fit to describe MF from patterns modulated by non-focusing array elements like amplitude meshes and by reflective spatial modulators.

Acknowledgments This project was supported by 973 program (2013CB922404); National Natural Science Foundation of China under Grant Nos. 11274053, 11474039, 11474040, 11004240 and 61178022; the Research Fund for the Doctoral Program of Higher Education of China Under Grant Nos. 20122216120009 and 20122216110007; and funds from the Science and Technical Department of Jilin Province under Grant No. 20130522149JH.

References

1. A. Braun, G. Korn, X. Liu, D. Du, J. Squier, G. Mourou, Self-channeling of high-peak-power femtosecond laser pulses in air. Opt. Lett. **20**(1), 73–75 (1995)
2. O.G. Kosareva, V.P. Kandidov, A. Brodeur, C.Y. Chien, S.L. Chin, Conical emission from laser-plasma interactions in the filamentation of powerful ultrashort laser pulses in air. Opt. Lett. **22**(17), 1332–1334 (1997)
3. S. Tzortzakis, B. Prade, M. Franco, A. Mysyrowicz, S. Hüller, P. Mora, Femtosecond laser-guided electric discharge in air. Phys. Rev. E **64**, 057401 (2001)
4. S. Tzortzakis, G. Méchain, G. Patalano, Y.-B. André, B. Prade, M. Franco, A. Mysyrowicz, J.-M. Munier, M. Gheudin, G. Beaudin, P. Encrenaz, Coherent subterahertz radiation from femtosecond infrared filaments in air. Opt. Lett. **27**(21), 1944–1946 (2002)
5. P. Rohwetter et al., Laser-induced water condensation in air. Nat. Photon. **4**, 451 (2010)
6. G. Fibich, B. Ilan, Deterministic vectorial effects lead to multiple filamentation. Opt. Lett. **26**(11), 840–842 (2001)
7. K.M. Guo, J.Q. Lin, Z.Q. Hao, X. Gao, Z.M. Zhao, C.K. Sun, B.Z. Li, Triggering and guiding high-voltage discharge in air by single and multiple femtosecond filaments. Opt. Lett. **37**, 259–261 (2012)
8. A. Camino, Z.Q. Hao, X. Liu, J.Q. Lin, High spectral power femtosecond supercontinuum source by use of a microlens array. Opt. Lett. **39**(4), 747–750 (2014)
9. M. Alshershby, Z.Q. Hao, A. Camino, J.Q. Lin, Modeling a femtosecond filament array waveguide for guiding pulsed infrared laser radiation. Opt. Commun. **296**, 87–94 (2013)
10. N. Jhajj, E.W. Rosenthal, R. Birnbaum, J.K. Wahlstrand, H.M. Milchberg, Demonstration of long-lived high-power optical waveguides in air. Phys. Rev. X **4**, 011027 (2014)
11. Y. Ren, M. Alshershby, Z.Q. Hao, Z.M. Zhao, J.Q. Lin, Microwave guiding along double femtosecond filaments in air. Phys. Rev. E **88**, 013104 (2013)
12. A. Dubietis, G. Tamošauskas, G. Fibich, B. Ilan, Multiple filamentation induced by input-beam ellipticity. Opt. Lett. **29**(10), 1126–1128 (2004)
13. T.D. Grow, A.L. Gaeta, Dependence of multiple filamentation on beam ellipticity. Opt. Expr. **13**(12), 4594–4599 (2005)
14. J.S. Liu, H. Schroeder, S.L. Chin, R.X. Li, Z.Z. Xu, Ultrafast control of multiple filamentation by ultrafast laser pulses. Appl. Phys. Lett. **87**, 161105 (2005)
15. T.D. Grow, A.A. Ishaaya, L.T. Vuong, A.L. Gaeta, N. Gavish, G. Fibich, Collapse dynamics of super-Gaussian beams. Opt. Express **14**(12), 5468–5475 (2006)
16. A. Camino, Z.Q. Hao, X. Liu, J.Q. Lin, Control of laser filamentation in fused silica by a periodic microlens array. Opt. Express **21**(7), 7908–7915 (2013)
17. Z.Q. Hao, K. Stelmaszczyk, P. Rohwetter, W.M. Nakaema, L. Woeste, Femtosecond laser filament-fringes in fused silica. Opt. Express **19**(8), 7799–7806 (2011)
18. H. Schroeder, J. Liu, S.L. Chin, From random to controlled small-scale filamentation in water. Opt. Express **12**(20), 4768–4774 (2004)
19. H. Gao, W. Chu, G.L. Yu, B. Zeng, J.Y. Zhao, Z. Wang, W.W. Liu, Y. Cheng, Z.Z. Xu, Femtosecond laser filament array generated with step phase plate in air. Opt. Express **21**(4), 4612–4622 (2013)
20. G. Méchain, A. Couairon, M. Franco, B. Prade, A. Mysyrowicz, Organizing multiple femtosecond filaments in air. Phys. Rev. Lett. **93**(3), 035003 (2004)
21. Z.Q. Hao, J. Zhang, T.T. Xi, X.H. Yuan, Z.Y. Zheng, X. Lu, M.Y. Yu, Y.T. Li, Z.H. Wang, W. Zhao, Z.Y. Wei, Optimization of multiple filamentation of femtosecond laser pulses in air using a pinhole. Opt. Express **15**(24), 16102–16109 (2007)
22. O.G. Kosareva, N.A. Panov, N. Akozbek, V.P. Kandidov, Q. Luo, S.A. Hosseini, W. Liu, J.-F. Gravel, G. Roy, S.L. Chin, Controlling a bunch of MF by means of a beam diameter. Appl. Phys. B **82**, 111–122 (2006)
23. P. Rohwetter, M. Queißer, K. Stelmaszczyk, M. Fechner, L. Wöste, Laser multiple filamentation control in air using a smooth phase mask. Phys. Rev. A **77**, 013812 (2008)
24. C.P. Hauri, J. Gautier, A. Trisorio, E. Papalazarou, P. Zeitoun, Two dimensional organization of a large number of stationary optical filaments by adaptive wave front control. Appl. Phys. B **90**, 391–394 (2008)
25. J. Yu, D. Mondelain, J. Kasparian, E. Salmon, S. Geffroy, C. Favre, V. Boutou, J.-P. Wolf, Sonographic probing of laser filaments in air. Appl. Opt. **42**(36), 7117–7120 (2003)
26. T.T. Xi, Z.J. Zhao, Z.Q. Hao, Femtosecond laser filamentation with microlens array in air. J. Opt. Soc. Am. B **32**, 163–166 (2015)
27. M. Berry, I. Marzoli, W. Schleich, Quantum carpets, carpets of light. Phys. World **June 2001**, 39–46 (2001)
28. M. Mlejnek, E.M. Wright, J.V. Moloney, Dynamic spatial replenishment of femtosecond pulses propagating in air. Opt. Lett. **23**(5), 382–384 (1998)
29. A.A. Dergachev, A.A. Ionin, V.P. Kandidov, D.V. Mokrousova, L.V. Seleznev, D.V. Sinitsyn, E.S. Sunchugasheva, S.A. Shlenov, A.P. Shustikova, Plasma channels during filamentation of a femtosecond laser pulse with wavefront astigmatism in air. Quantum Electron. **44**(12), 1085–1090 (2014)
30. S. Henin, Y. Petit, J. Kasparian, J.-P. Wolf, A. Jochmann, S.D. Kraft, S. Bock, U. Schramm, R. Sauerbrey, W.M. Nakaema, K. Stelmaszczyk, P. Rohwetter, L. Wöste, C.-L. Soulez, S. Mauger, L. Bergé, S. Skupin, Saturation of the filament density of ultrashort intense laser pulses in air. Appl. Phys. B **100**, 77–84 (2010)